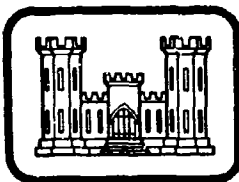


AD A101409



LEVEL #
12
BS



MISCELLANEOUS PAPER SL-81-4

CORRELATION OF MOBILITY CONE INDEX WITH FUNDAMENTAL ENGINEERING PROPERTIES OF SOIL

by

Behzad Rohani and George Y. Baladi

Structures Laboratory
U. S. Army Engineer Waterways Experiment Station
P. O. Box 631, Vicksburg, Miss. 39180

April 1981

Final Report

JUL 1 9 1981

A

Approved For Public Release; Distribution Unlimited



X DTIC FILE COPY

Prepared for Office, Chief of Engineers, U. S. Army
Washington, D. C. 20314

Under Project 4AI61102AT22, Task CO, Work Unit 001

Monitored by Geotechnical Laboratory
U. S. Army Engineer Waterways Experiment Station
P. O. Box 631, Vicksburg, Miss. 39180

81 7 14 006

**Destroy this report when no longer needed. Do not return
it to the originator.**

**The findings in this report are not to be construed as an official
Department of the Army position unless so designated,
by other authorized documents.**

**The contents of this report are not to be used for
advertising, publication, or promotional purposes.
Citation of trade names does not constitute an
official endorsement or approval of the use of
such commercial products.**

Unclassified

~~SECURITY CLASSIFICATION OF THIS PAGE (Line Ref ID: A6119)~~

DD FORM 1 JAN 73 1473 EDITION OF 1 NOV 68 IS OBSOLETE

Unclassified

SECURITY CLASSIFICATION OF THIS PAGE (When Data Entered)

Unclassified

SECURITY CLASSIFICATION OF THIS PAGE(When Data Entered)

20. ABSTRACT (Continued)

O.S Sq in.

Recent developments in analytical modeling of vehicle performance require that the soil be described in terms of its fundamental properties such as angle of internal friction, cohesion, stiffness, density, etc. In order to utilize the larger CI data base and establish correspondence between the empirical studies and theoretical mobility models, it was necessary to correlate CI with the engineering properties of soil.

This paper describes the development of a mathematical model that treats the cone penetration process as expansion of a series of spherical cavities, simulating the geometry of the cone, in an elastic-plastic isotropic medium. The stresses required to expand these cavities are integrated over the surface area of the cone in order to determine the forces resisting the penetration of the cone, in terms of the fundamental engineering properties of soil. Analytical predictions are made for the standard WES cone penetrometer, which is a 30-degree, right-circular cone of 0.542 in. base area, and the results are compared with experimental data for various types of soil. The results achieved indicate good agreement between CI and basic engineering soil properties.

Unclassified

SECURITY CLASSIFICATION OF THIS PAGE(When Data Entered)

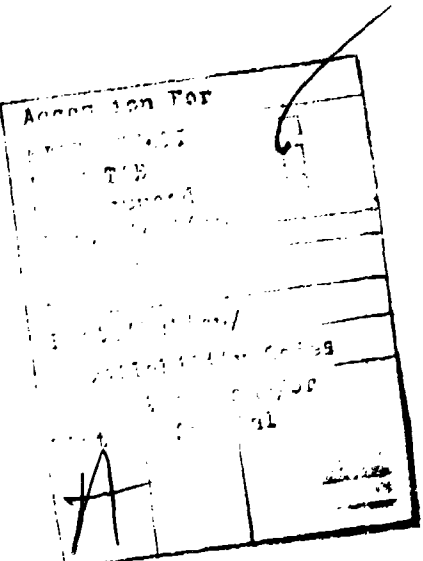
PREFACE

This paper was prepared for presentation at the Seventh International Congress of the International Society for Terrain-Vehicle Systems, 16-20 August 1981, in Calgary, Canada.

The investigation was conducted for the Office, Chief of Engineers, U. S. Army, by personnel of the Geomechanics Division (GD), Structures Laboratory (SL), U. S. Army Engineer Waterways Experiment Station (WES), as a part of Project 4A161102AT22, "Dynamic Soil-Track Interactions Governing High-Speed Combat Vehicle Performance."

This study was conducted by Drs. Behzad Rohani and George Y. Baladi during the period October 1980 - January 1981 under the general direction of Mr. Bryant Mather, Chief, SL; Dr. J. G. Jackson, Jr., Chief, GD; and Mr. C. J. Nuttall, Jr., Chief, Mobility Systems Division, Geotechnical Laboratory. The paper was written by Drs. Rohani and Baladi.

LTC David C. Girardot, Jr., CE, was Acting Commander of WES during the investigation. Mr. F. R. Brown was Acting Director.



CONTENTS

	<u>Page</u>
PREFACE	1
PART I: INTRODUCTION	3
PART II: DERIVATION OF THE CONE PENETRATION MODEL	5
Formulation of the Problem	5
Stresses Resisting the Motion of the Cone	5
Cone Index Equation	7
Free-Surface Effect	8
PART III: PARAMETER STUDY OF THE EFFECT OF SOIL PROPERTIES AND CONE APEX ANGLE ON CI	10
Part A: Clay Soil	10
Part B: Sand	10
Part C: Mixed Soil	14
Part D: Effect of Cone Apex Angle on CI	14
PART IV: COMPARISON OF PREDICTED AND MEASURED CONE INDEX	18
Comparison with Clay Soil	18
Comparison with Mixed Soil	20
Comparison with Sand	20
PART V: SUMMARY AND RECOMMENDATIONS	27
REFERENCES	28
APPENDIX A: TREATMENT OF LAYERED SOIL	A1
APPENDIX B: NOTATION	B1

CORRELATION OF MOBILITY CONE INDEX WITH
FUNDAMENTAL ENGINEERING PROPERTIES OF SOIL

PART I: INTRODUCTION

1. Cone index (CI) has been used successfully by the U. S. Army Engineer Waterways Experiment Station (WES) as a descriptor of soil strength in establishing empirical soil-vehicle relations for predicting the performance of ground-crawling vehicles (Reference 1). CI is a measure of the resistance of the soil to the penetration of a right-circular cone.* Although used as an undimensioned index, CI is actually the number of pounds of force exerted on the handle of the penetrator divided by the area of the cone base in square inches. The embedding process is usually neglected in practice and the first CI reading is taken when the cone is fully embedded. For off-the-road mobility applications the depth of interest for CI measurements seldom exceeds 2 ft. Readings are taken for depth increments of 1 in. and are often averaged over the depth of interest in order to describe the strength of the soil by a single CI number. In cases where CI varies significantly with depth (e.g., in the case of dense sand), the data are sometimes displayed graphically, showing the variation of CI with depth of penetration.

2. Recent developments in analytical modeling of vehicle performance require that the soil be described in terms of its fundamental mechanical properties such as angle of internal friction, cohesion, density, etc. In order to utilize the larger CI data base and establish correspondence between the empirical studies and theoretical mobility models, it is necessary to correlate CI with the engineering properties of soil.

3. There are several solutions to cone and wedge penetration problems available in the literature (e.g., References 2 and 3). These solutions are based on the theory of rigid plasticity and do not account for the stiffness characteristic of the soil. Experimental data, however, indicate that CI does not depend solely on the shear strength parameters but also depends on the stiffness characteristic of soil. This paper describes the development of a simplified mathematical model for the cone penetration process for the

* In practice, the rate of penetration is on the order of 1.2 in./sec.

correlation of CI with the fundamental engineering properties of soil, taking into consideration the stiffness characteristic of the material. The basic premise of the model is the assumption that the cone penetration process in earth materials can be viewed as the expansion of a series of spherical cavities (simulating the geometry of the cone) in an elastic-plastic medium. The normal stress (normal to the surface of the cone) resisting the penetration of the cone is therefore equivalent to the internal pressure required for the expansion of a spherical cavity in an elastic-plastic material. Using this expression for the internal pressure, the vertical force resisting the penetration of the cone is computed from the geometry of the cone and conditions of static equilibrium. In order to demonstrate the application of the model, analytical predictions are made for the standard WES cone penetrometer and the results are compared with experimental data for various types of soil. Analysis of cone penetration in layered media is presented in Appendix A.

PART II: DERIVATION OF THE CONE PENETRATION MODEL

Formulation of the Problem

4. The basic geometry of the problem is depicted in Figure 1a. A cone of diameter D , length L , and apex angle 2α is penetrating a rate-independent isotropic medium, satisfying the Mohr-Coulomb failure condition. The tip of the cone is located at a distance $2+L$ from the surface of the medium. The state of stress for a finite frustum of the cone at depth $Z+L-\eta$ is shown in Figure 1b, where σ and τ are the normal and shear stresses resisting the motion of the cone, respectively. Integration of these stresses over the surface of the cone will determine the magnitude of the vertical force F_z (Figure 1a) that must be exerted on the shaft of the cone in order to penetrate the soil. However, σ and τ are not known a priori. In order to make the problem tractable these stresses must be related and expressed in terms of the fundamental properties of soil.

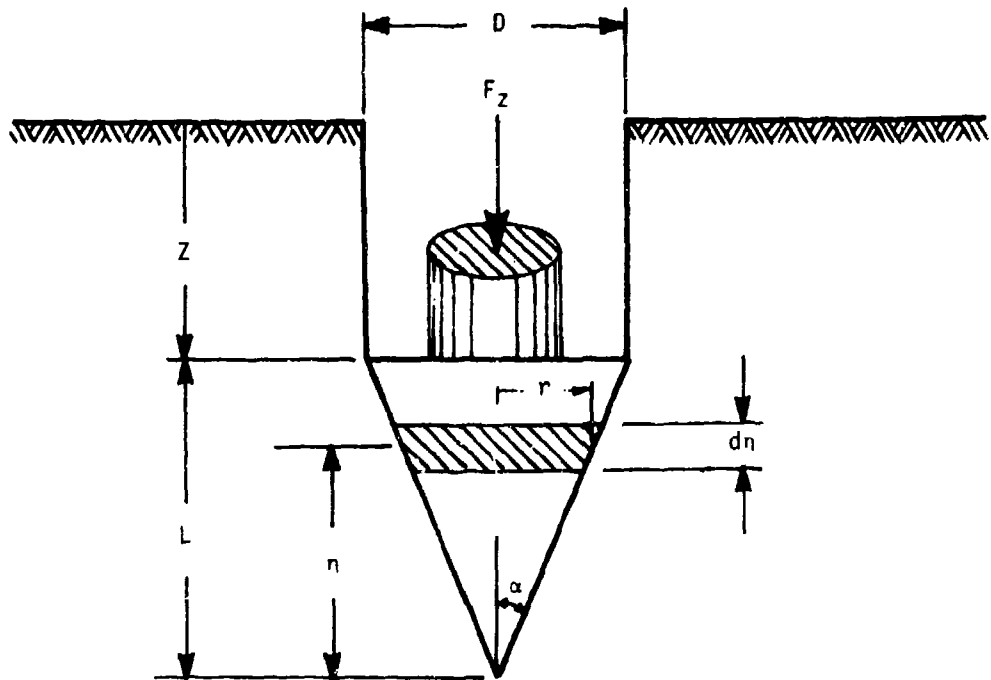
Stresses Resisting The Motion of the Cone

5. It has been observed in practice that the cone has a tendency to shear the surrounding material during the penetration process. This indicates that the entire shearing strength of the soil is mobilized in resisting the motion of the cone. The shear stress τ can therefore be expressed as

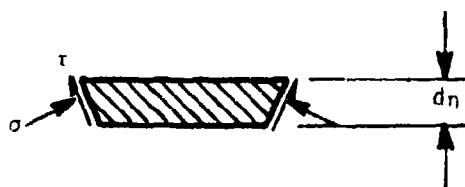
$$\tau = C + \sigma \tan \phi \quad (1)$$

where C = cohesion and ϕ = angle of internal friction. As was pointed out previously, the normal stress σ is assumed to be equivalent to the internal pressure required to expand a spherical cavity in an elastic-plastic material (Figure 1c). The expression for the internal pressure for an expanding spherical cavity in an unbounded elastic-plastic medium is (Reference 4)

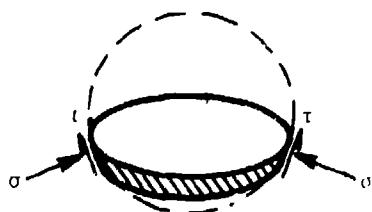
$$\sigma = 3(q + C \cot \phi) \left(\frac{1 + \sin \frac{\phi}{2}}{3 - \sin \phi} \right) \left(\frac{\tilde{G}}{C + q \tan \phi} \right)^{\frac{4 \sin \phi}{3(1 + \sin \phi)}} - C \cot \phi \quad (2)$$



(a) Geometry of the problem



(b) Stresses on a finite frustum of the cone



(c) Analogy between cavity expansion and cone penetration process

Figure 1. The cone penetration problem

According to Reference 4, Equation 2 was obtained for the condition $\tan \phi > 0$. For cohesive soils, where $\tan \phi = 0$, Reference 4 gives the following expression for σ

$$\sigma = \frac{4}{3} C \left(1 + \ln \frac{\tilde{G}}{C} \right) + q \quad (3)$$

where q = in situ hydrostatic stress and \tilde{G} = apparent shear modulus which will be discussed subsequently. The in situ hydrostatic stress corresponding to the depth $Z+L-\eta$ (Figure 1a) is given as

$$q = (Z+L-\eta)\gamma \quad (4)$$

where γ = density. The quantities $\tilde{G}/(C + q \tan \phi)$ and \tilde{G}/C in Equations 2 and 3 express the ratio of the shear modulus to shear strength of the material and are referred to as rigidity index. Equations 1 through 3 are generic expressions for the stresses resisting the motion of the cone in terms of the soil parameters C , ϕ , γ , and \tilde{G} and the depth $Z+L-\eta$.

Cone Index Equation

6. From the geometry of the problem (Figure 1a) and conditions of static equilibrium, the resistive force F_z becomes

$$F_z = \int_0^L (\sigma \tan \alpha + \tau) 2\pi r d\eta \quad (5)$$

where $r = \eta \tan \alpha$. By definition, CI is given as

$$CI = \frac{4F_z}{\pi D^2} \quad (6)$$

Combining Equations 1, 2, 5, and 6 and completing the integration for F_z , we obtain the following general expression for CI:

$$CI = -C \cot \phi + \frac{2 \tan \alpha (1 + \sin \phi) C^m}{\left(\frac{D}{2} \gamma\right)^2 \tan^3 \phi} \left[\frac{3(\tan \alpha + \tan \phi)}{3 - \sin \phi} \right]_0$$

where

$$\Omega = \frac{[C + \gamma(Z+L)\tan\phi]^{3-m} - [C + \gamma(Z+L)\tan\phi + (2-m)\gamma L \tan\phi](C + \gamma Z \tan\phi)^{2-m}}{(2-m)(3-m)}$$

For granular materials $C = 0$ and Equation 7 reduces to

$$CI = \frac{2 \tan \alpha (1 + \sin \phi) C^m}{\left(\frac{D}{2} \gamma\right)^2 \tan^3 \phi} \left[\frac{3(\tan \alpha + \tan \phi)}{3 - \sin \phi} \right]_0$$

where

$$\Omega = \frac{[\gamma(Z+L)\tan\phi]^{3-m} - [\gamma(Z+L)\tan\phi + (2-m)\gamma L \tan\phi](\gamma Z \tan\phi)^{2-m}}{(2-m)(3-m)}$$

For cohesive soil where $\tan \phi = 0$, the expression for CI can be obtained by combining Equations 1, 3, 5, and 6 and completing the integration for F_z . Thus for cohesive soil

$$CI = \frac{4}{3} C(1 + \ln \frac{\bar{d}}{C}) + \frac{2L}{D} C + \gamma(Z + L/3) \quad (9)$$

In Equations 7 through 9, $m = 4 \sin \phi / 3(1 + \sin \phi)$ and $Z = 0$ where $Z < 0$ corresponds to fully embedded cones (Figure 1a). Equation 9 is similar to the expressions reported in Reference 5 for cone penetration analysis in clays. Equations 7 through 9 express the cone index CI in terms of the soil parameters C , ϕ , γ , and \bar{d} , the depth of penetration Z , and the geometry of the cone.

Free-Surface Effect

7. The normal stress σ (Equations 2 and 4) which was used to derive the CI expressions is for the expansion of a cavity in an unbounded medium. The process of cone penetration, however, takes place in a medium which is bounded by a free surface. The existence of this free boundary will result in an upward flow of the near-surface materials in the vicinity of the cone

and, consequently, reduces the penetration resistance of the cone. The free-surface effect is most pronounced for granular materials and becomes less important as the cohesive strength of the material increases. Also, its effect on cone penetration resistance decreases with depth and eventually becomes negligible. In the case of the standard WES cone it appears that at a depth of about 6L the effect of free surface on the penetration resistance in sand becomes negligible. To account for the free-surface effect for granular materials it is postulated that the apparent shear modulus \tilde{G} which controls the shearing flow of the material varies with depth according to the following relation

$$\tilde{G} = 0.5 \left[A + \frac{B - B \exp(-\beta Z)}{1 + B \exp(-\beta Z)} \right] G \quad (10)$$

where A , B , β , and G are constants that must be evaluated experimentally. The constants A , B , and β are independent of soil type and are related to the size of the cone of interest. The constant G is the actual static shear modulus and depends on soil type and the initial state of compaction of the material. In the case of cohesive or mixed soil, free-surface effect is negligible. In this case the constants in Equation 10 become $A = 1$, $B = 0$, and $\beta = 0$ (i.e., $\tilde{G} = G$). The numerical values of the three constants A , B , and β have been determined for granular materials (for the standard WES cone) and are tabulated below:

$$A = 0.986$$

$$B = 100$$

$$\beta = 0.55 (\text{in.})^{-1}$$

Comparisons of the experimental data and theoretical predictions presented in the last section of the paper demonstrate the validity of Equation 10. It is believed that the numerical values of the coefficients A , B , and β given in the above tabulation are also applicable to cones that are blunter than the standard WES cone (i.e., apex angles greater than 30 degrees). This is probably true since G is only mildly dependent on the apex angle (see Figure 6).

PART III: PARAMETER STUDY OF THE EFFECT OF
SOIL PROPERTIES AND CONE APEX ANGLE ON CI

8. The effects of various soil parameters and the cone apex angle on CI are studied parametrically in this section. The study is divided into four parts: (a) clay soil, (b) sand, (c) mixed soil, and (d) effect of cone apex angle on CI. The standard WES cone ($L = 1.48$ in. and $D = 0.799$ in.) is used for the parameter studies in Parts A through C. In Part D, the length of the cone was kept constant (i.e., $L = 1.48$ in.) and the diameter was varied to produce different apex angles. For all calculations $\gamma = 0.06$ lb/in.³.

Part A: Clay Soil

9. The variation of cone index with cohesion for clay soils is shown in Figure 2 for a rigidity index range of 10 to 500. The cone index is calculated for two different depths (i.e., $Z = 2L$ and $Z = 10L$). It is clear from Figure 2 that for the shallow depths considered in this study CI is independent of depth. Figure 2 also indicates that the CI does not depend solely on the cohesion of the material. For a given value of cohesion CI increases with increasing rigidity index G/C (or shear modulus G). The dependency of CI on G, however, is relatively weak. For the particular cone and the depths of interest considered in this study, CI increases from about 8.5C to 14C due to an increase of a factor of 50 in the value of G. Examination of Equation 9 indicates that in general the variation of CI with cohesion depends on the size of the cone, the depth of penetration, and the three soil parameters C, G, and γ .

Part B: Sand

10. The expression for the cone index for sand is given in Equation 8 with the apparent shear modulus \tilde{G} defined by Equation 10. These equations are used to study the effect of the angle of internal friction on cone index. The results of the calculations are shown in Figures 3 and 4 for $Z/L = 2$ and $Z/L = 10$, respectively. Figures 3 and 4 indicate that for granular materials the cone index does not depend solely on the angle of internal friction. For a given friction angle ϕ the cone index increases

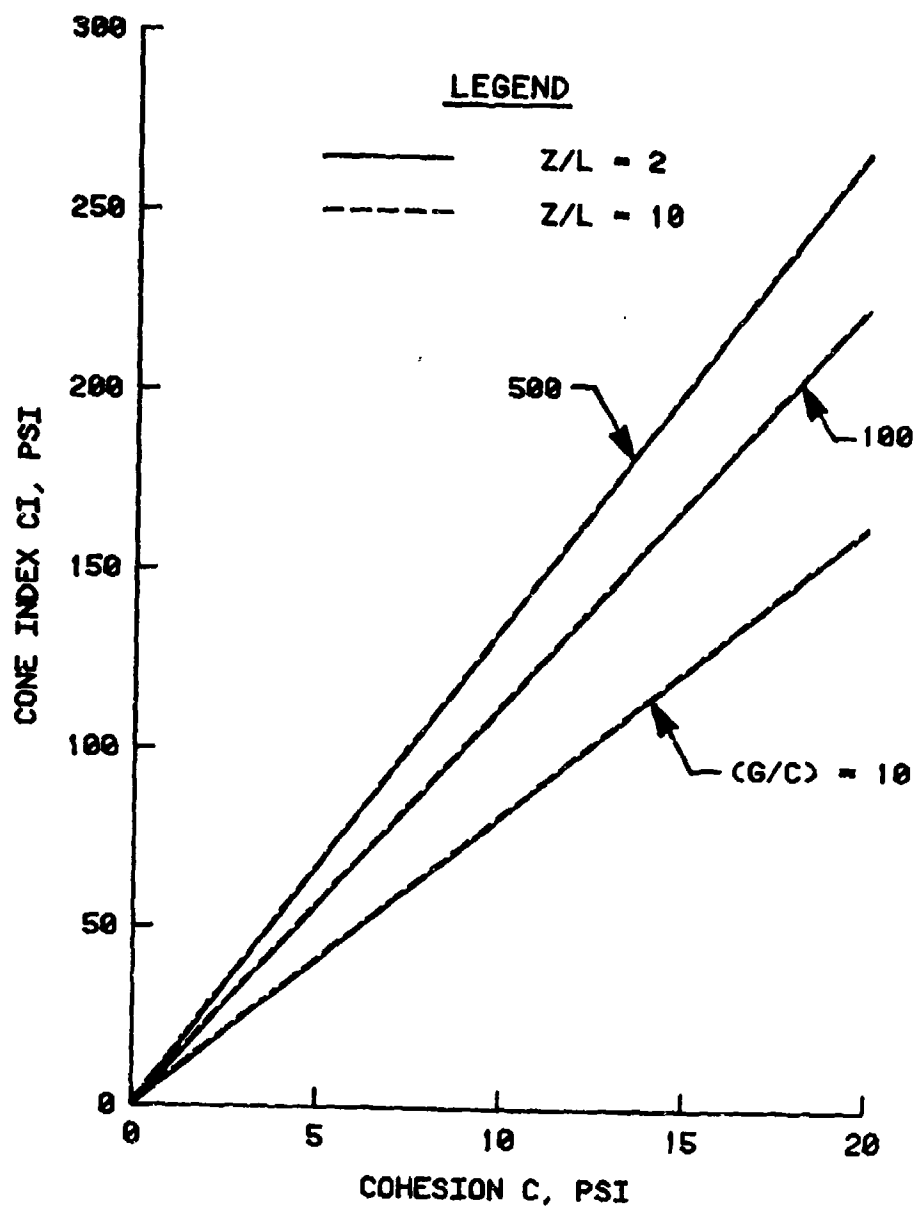


Figure 2. Variation of cone index with cohesion for $\phi = 0$ material

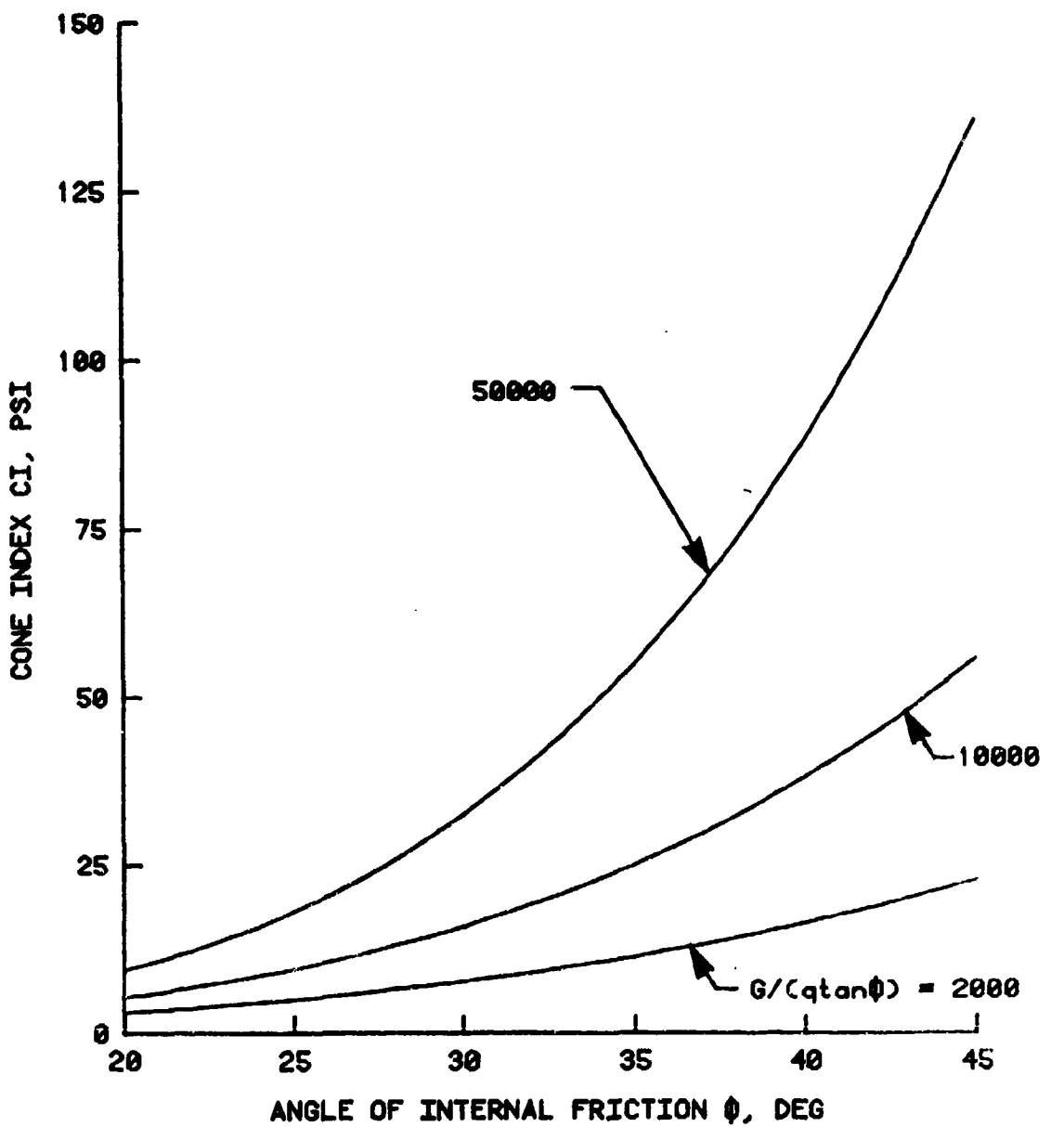


Figure 3. Variation of cone index with angle of internal friction for $C = 0$ material ($Z/L = 2$)

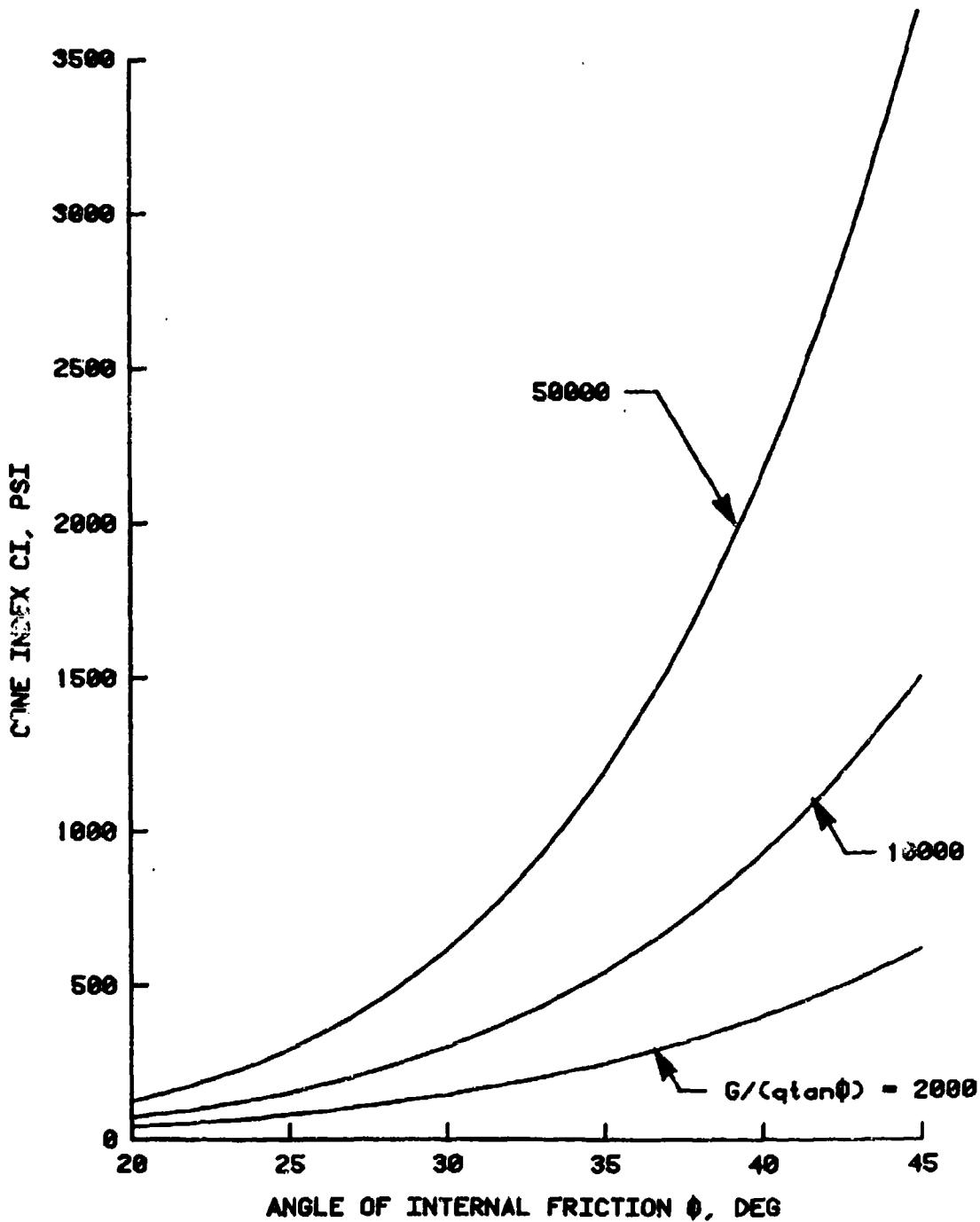


Figure 4. Variation of cone index with angle of internal friction for $C = 0$ material ($Z/L = 10$)

with increasing rigidity index. The dependency of CI on rigidity index (or shear modulus), however, is not very strong for low friction angles. As the friction angle increases this dependency becomes stronger. For example, for $\phi = 45$ degrees, increasing the shear modulus by a factor of 25 would increase the cone index by approximately a factor of 6. The same increase in the shear modulus would result in an increase of about a factor of 3 in the value of CI for $\phi = 20$ degrees. The most interesting feature of the relationships in Figures 3 and 4 is the strong dependency of the cone index on the angle of internal friction, particularly for the higher values of the rigidity index. Comparison of Figures 3 and 4 also indicates the strong dependency of the cone index on depth of penetration for granular materials.

Part C: Mixed Soil

11. The result from a series of calculations for a mixed soil ($C = 5$ psi, $\phi = 20$ degrees) is presented in Figure 5 in terms of cone index versus normalized depth of penetration Z/L . Also shown in Figure 5 are corresponding curves for a clay soil ($C = 5$ psi, $\phi = 0$ degree) and a granular material ($C = 0$ psi, $\phi = 20$ degrees). The effect of the coupling of the cohesion and angle of internal friction on the cone index is clearly demonstrated in Figure 5. For the depths of interest and the values of C and ϕ considered in this study, Figure 5 indicates that for the mixed soil the cone index is about 2.5 to 4.5 times the sum of the cone indices for the $C = 5$ psi, $\phi = 0$ degree and $C = 0$ psi, $\phi = 20$ degrees soils. Also, as expected, the variation of CI with depth for a mixed soil is not as pronounced as that for a granular material.

Part D: Effect of Cone Apex Angle on CI

12. The variation of CI with cone apex angle is shown in Figure 6 for three different soils at a normalized depth of $Z/L = 10$. These graphs were obtained by keeping the length of the cone constant ($L = 1.48$ in.) and varying the diameter to produce various apex angles. The apex angle for the standard WES cone is $2\alpha = 30$ degrees. As depicted in Figure 6, CI increases with decreasing apex angle for all soils considered. The rate of increase is very pronounced for apex angles smaller than 30 degrees. This range of

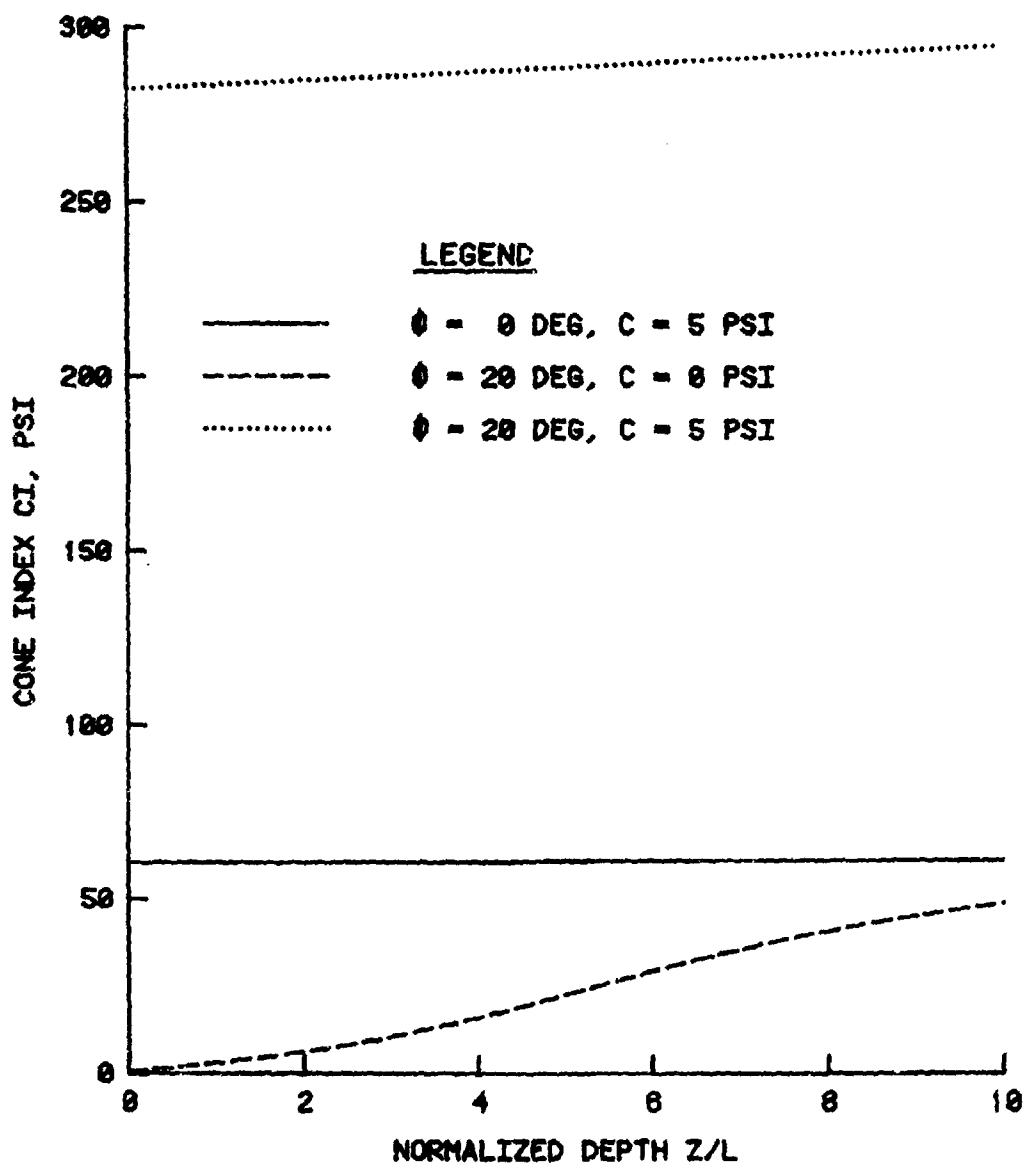


Figure 5. Variation of cone index with depth

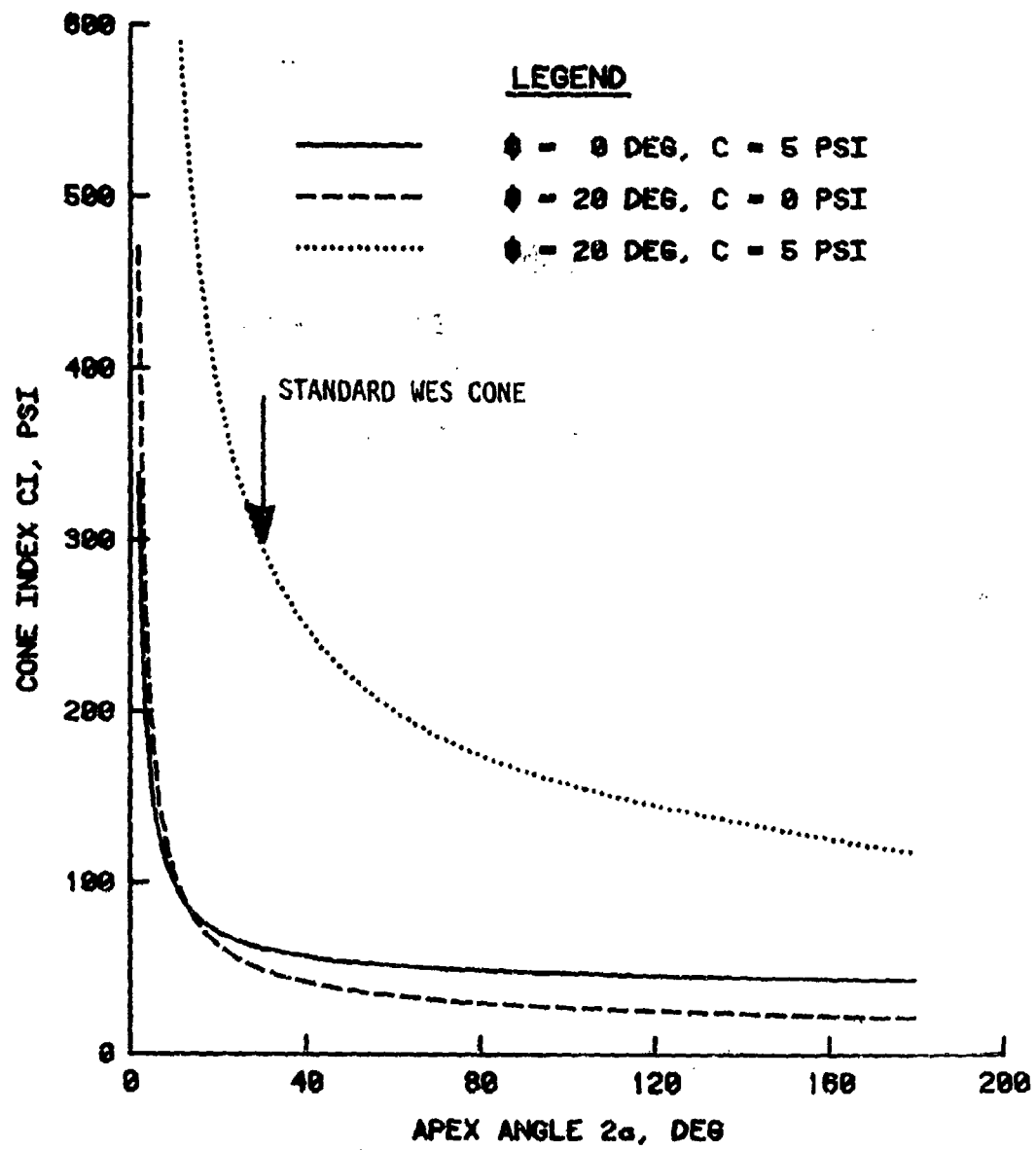


Figure 6. Variation of cone index with apex angle of cone
(Z/L = 10)

apex angles, however, is not of practical interest. For apex angles greater than 30 degrees, the variation of CI with apex angle is least pronounced for clay and most pronounced for mixed soil. For clay soil CI increases by approximately 50 percent as the apex angle is reduced from 180 to 30 degrees. For the same change in the apex angle, CI increases by a factor of approximately 2.5 in the case of mixed soil and a factor of 2 for sand. In general, however, the variation of CI with the apex angle is not unique and depends on the depth of penetration and the soil parameters C , ϕ , γ , and G .

PART IV: COMPARISON OF PREDICTED AND MEASURED CONE INDEX

13. In order to demonstrate the application of the cone penetration model, analytical predictions are made for the standard WES cone penetrometer and the results are compared with experimental data for various types of soil. Three different soils are considered for the comparison, i.e., clay soil, mixed soil, and sand. The results are discussed in the following paragraphs.

Comparison with Clay Soil

14. The results of a number of cone penetration tests for a lean clay and a heavy clay classified (according to the Unified Soil Classification System) as CL and CH, respectively, are documented in Reference 6. These tests were conducted in the laboratory under controlled conditions and provide an excellent means for evaluating the accuracy and range of application of the proposed cone index model. A summary of the test results is given in Table 1. The data provided in Reference 6 for each test consist of the values of cohesion, density, water content, and the average measured cone index. For each test bed five penetrations were made to a depth of about 5 in. and the results were averaged to obtain the cone index. The shear modulus of the soils used in the experiments was not measured. This parameter, however, is required for the theoretical prediction of CI. A literature search was conducted to determine typical values of shear modulus for materials similar to the clays tested in Reference 6. Based on the literature study a shear wave velocity of $V_s = \sqrt{Gg/\gamma} = 2100$ in./sec ($g =$ gravitational acceleration = 386.4 in./sec²) was selected for the clay soils from which the shear moduli given in Table 1 were calculated. These values of shear moduli are consistent with the values of Young's moduli obtained from results of triaxial tests conducted on lean clay from one of the test beds. The values of Young's moduli fall within the range of about 1200 to 2400 lb/in.². Furthermore, as was indicated in Figure 2, CI is not sensitive to G and reasonable uncertainties in G do not greatly affect the predicted value of CI.

Table 1
Cone Index Data for Clay ($\phi = 0$ Degree)

Test No.	Cohesion lb/in. ²	Density lb/in. ³	Shear Modulus lb/in. ²	Water Content %	Measured CI lb/in. ²	Predicted CI lb/in. ²
1	3.7	0.066	755	30.4	40	45
2	2.0	0.065	740	32.5	26	26
3	3.2	0.066	755	30.5	41	40
4	2.1	0.065	740	32.1	26	27
5	3.0	0.065	740	30.1	38	38
6	2.3	0.061	695	40.9	30	29
7	1.4	0.060	685	45.0	18	19
8	2.6	0.062	710	39.6	34	33
9	1.9	0.060	685	43.3	20	25
10	3.9	0.063	720	36.5	49	47
11	4.4	0.064	730	36.5	55	53
12	5.0	0.067	765	28.1	61	60
13	5.5	0.068	775	27.4	68	64
14	5.1	0.062	710	32.6	65	60
15	3.6	0.062	710	36.7	46	44

15. The values of cohesion, density, and shear modulus from Table 1 were used in Equation 9 for predicting CI for the clay soils. The results of the calculations are given in the last column of Table 1 and are also plotted against the measured CI in Figure 7. As shown in Figure 7, the predicted and measured values of CI are in excellent agreement.

Comparison with Mixed Soil

16. The results of cone penetration tests from Reference 6 for clays with small values of friction angles are given in Table 2. Similar to Table 1, the shear moduli given in Table 2 were obtained from a shear wave velocity of 175 ft/sec. The soil data in Table 2 were used in Equation 7 for predicting CI for this test series. The predicted results are given in the last column of Table 2 and are also plotted in Figure 8 against the measured values of CI. Again, the agreement between the predicted and measured CI is very good, although for the majority of the tests the predicted values are somewhat higher than the experimental data.

Comparison with Sand

17. The results of a series of laboratory cone penetration tests using the standard WES cone and three cohesionless soils are documented in Reference 7. The purpose of these tests was to establish empirical relations between cone penetration resistance and relative density. Therefore, for each sand, penetration tests were conducted at different relative densities and the results were presented in terms of CI versus depth of penetration. The results of these experiments provide a means for testing the validity of the concept of free-surface effect (Equation 10) and for evaluating the accuracy of the CI equation (Equation 8) for granular materials. Data for two sands at two different relative densities were selected for the study. The following tabulation shows the pertinent information for each test:

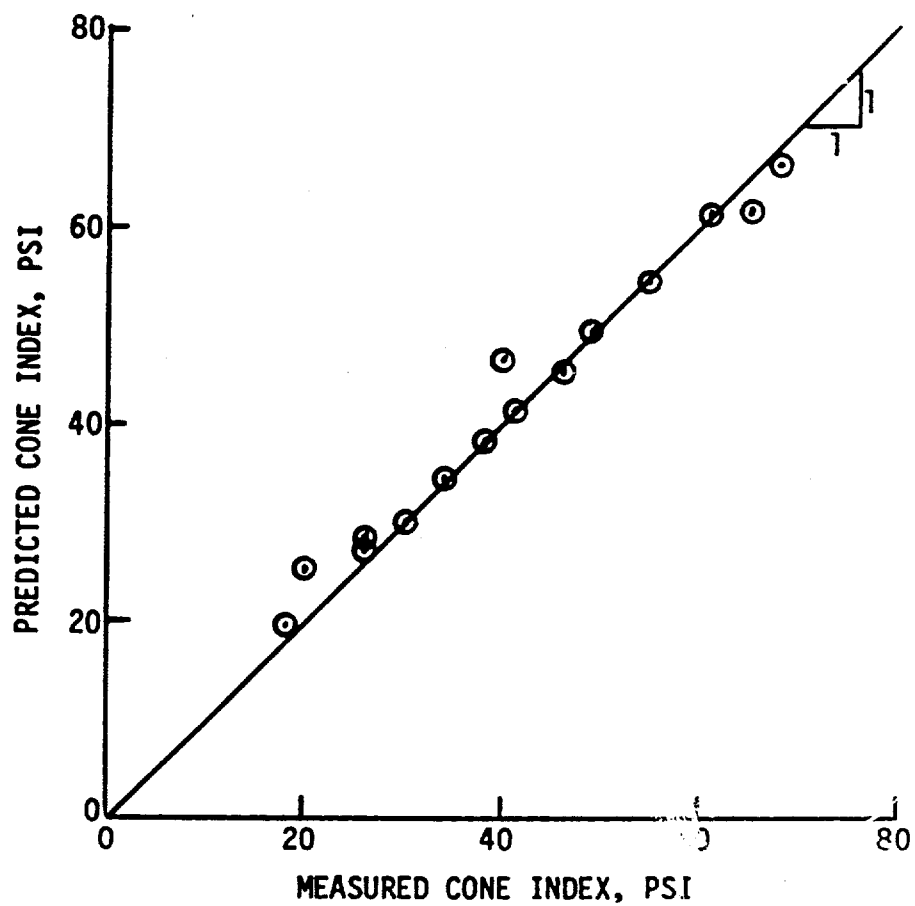


Figure 7. Comparison of predicted and measured cone index for clay ($\phi = 0$)

Table 2
Cone Index Data for Mixed Soil

Test No.	Cohesion 1b/in. ²	Friction Angle deg	Density 1b/in. ³	Shear Modulus 1b/in. ²	Water Content %	Measured CI 1b/in. ²	Predicted CI 1b/in. ²
1	5.0	17.5	0.062	710	22.0	206	217
2	5.6	13.0	0.063	720	22.7	183	174
3	4.5	9.5	0.063	720	24.5	126	115
4	3.5	10.0	0.066	755	26.9	100	100
5	5.5	7.0	0.064	730	25.9	86	111
6	6.8	17.5	0.065	740	22.3	236	269
7	7.0	11.5	0.067	765	24.1	172	187
8	7.5	15.5	0.067	765	22.3	270	256
9	5.5	8.5	0.059	675	29.4	98	122
10	6.8	12.5	0.058	660	24.9	161	188
11	5.5	10.0	0.065	740	30.2	127	140
12	9.5	11.0	0.065	740	25.1	188	224
13	10.2	12.5	0.064	730	25.4	222	258

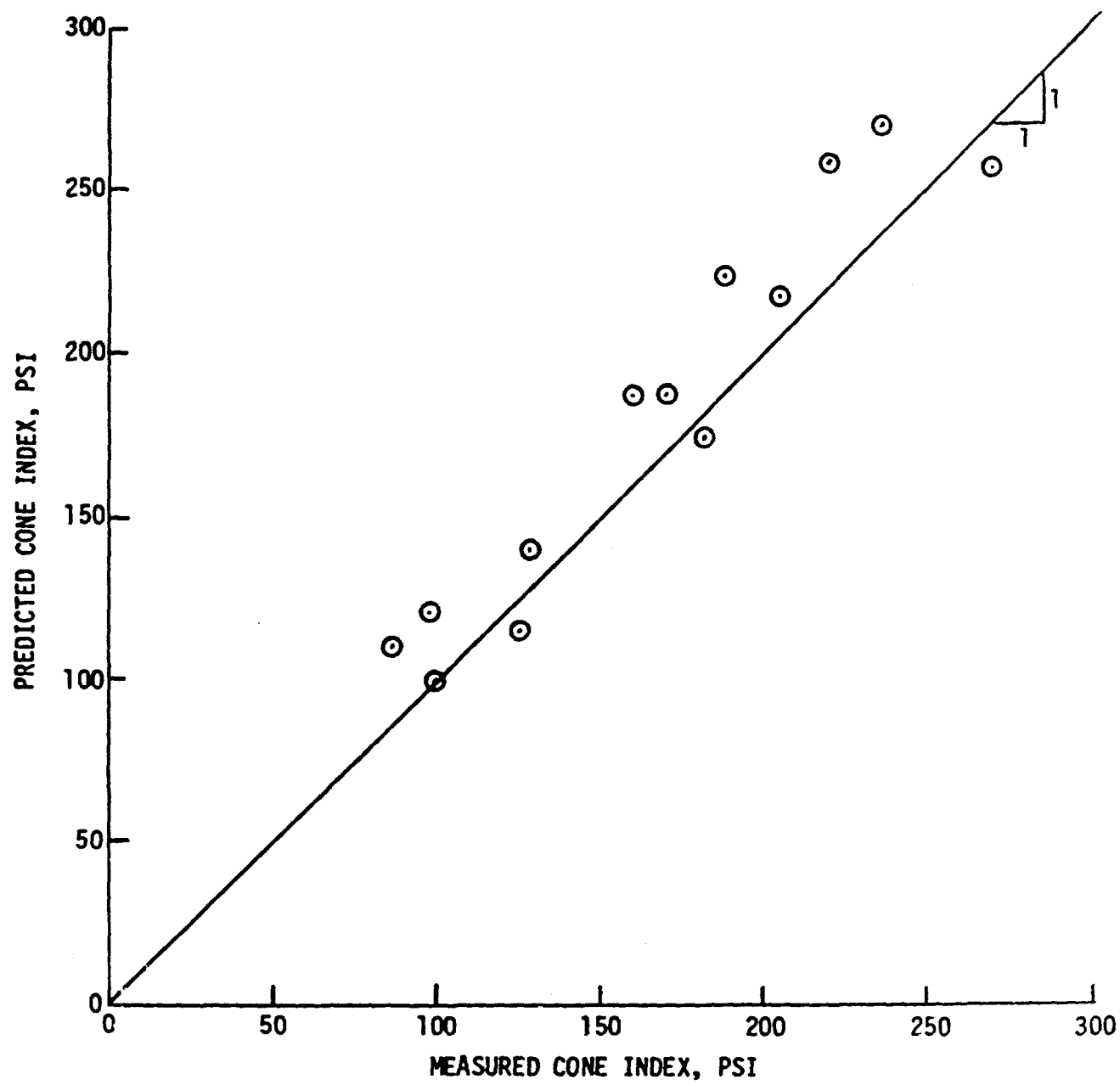


Figure 8. Comparison of predicted and measured cone index for mixed soil

<u>Test No.</u>	<u>Sand</u>	<u>Relative Density %</u>	<u>Friction Angle degrees</u>	<u>Density lb/in. ³</u>	<u>Shear Modulus* lb/in. ²</u>
1	Yuma (loose)	21.5	35	0.052	20
2	Yuma (Very Dense)	87.5	40	0.058	1000
3	Mortar (loose)	15.8	30	0.054	30
4	Mortar (Very Dense)	90.8	36	0.06	6800

* Estimated.

Yuma and mortar sands are uniformly graded fine sands and are classified (according to the Unified Soil Classification System) as SP-SM and SP, respectively. The actual CI versus depth relations for the four tests are shown in Figures 9 and 10. Figures 9 and 10 depict the strong dependency of CI on the initial state of compaction of sand. Also, in the case of dense sand, it is observed that CI is strongly dependent on the depth of penetration. In order to test the validity of the concept of free-surface effect, Equations 8 and 10 were first used to simulate the result of one of the tests and thus obtain the numerical values of the three constants A, B, and β in Equation 10. Using these constants, predictions were then made for the remaining three tests. The predicted CI versus depth relations are also plotted in Figures 9 and 10 for comparison with the experimental data. As observed from these figures the predicted and experimental curves compare very favorably, supporting the concept of free-surface effect. It should be pointed out that the shear moduli used for the calculations were obtained from literature and are considered as best estimate values for the materials of interest.

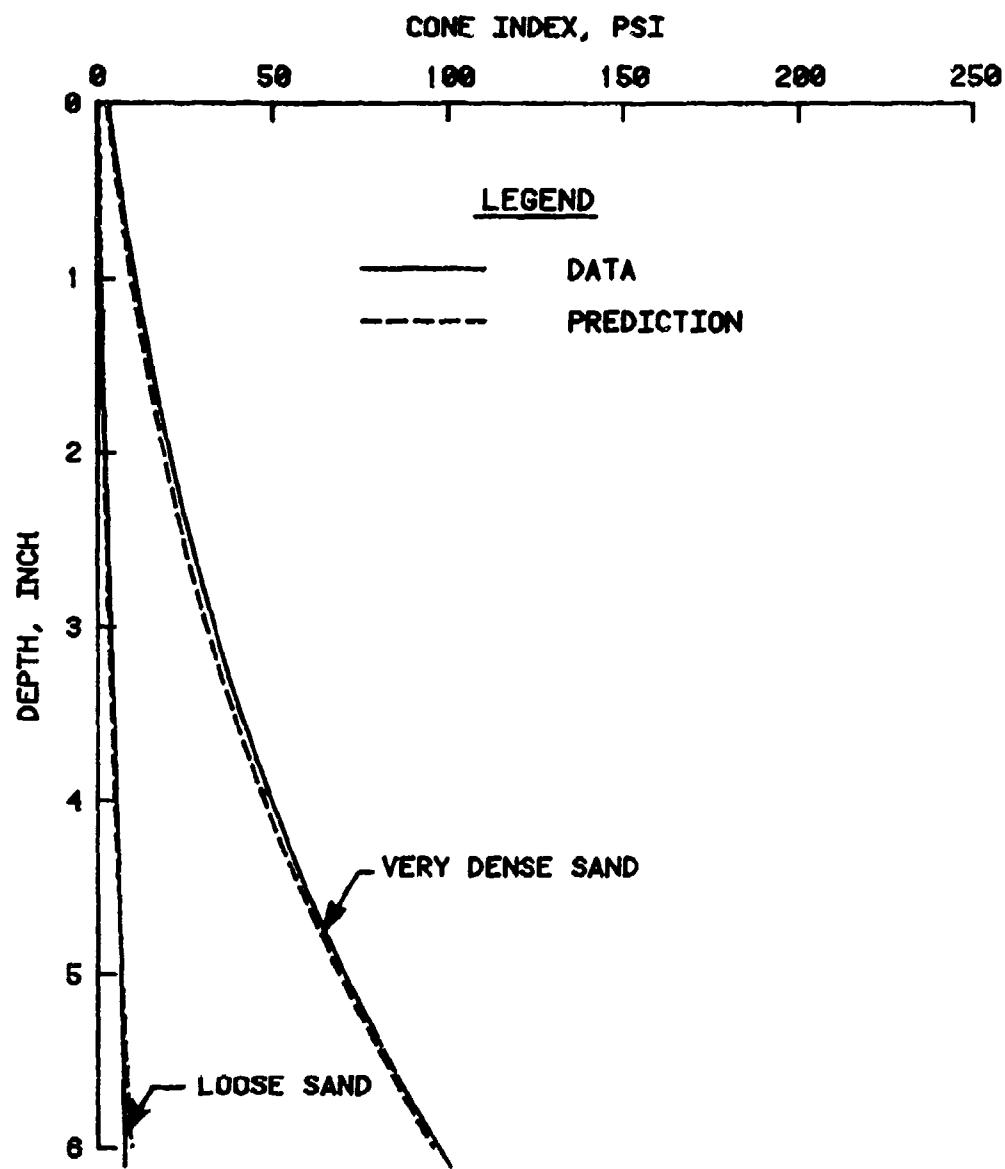


Figure 9. Cone index versus depth; measured data versus predictions for Yuma sand

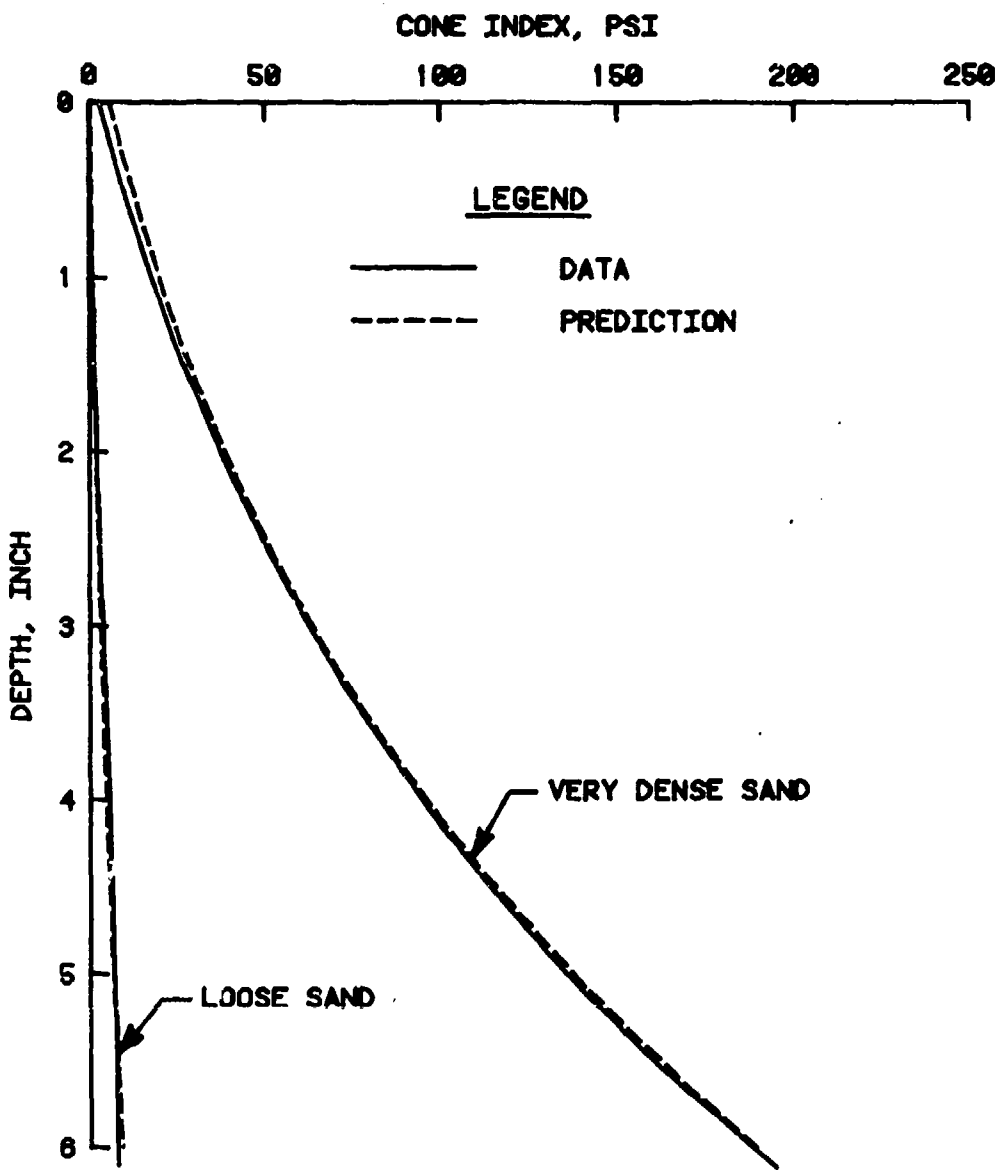


Figure 10. Cone index versus depth; measured data versus predictions for Mortar sand

PART V: SUMMARY AND RECOMMENDATIONS

18. A simplified cone penetration model based on spherical cavity expansion theory for an elastic-plastic medium has been developed and validated for the standard WES cone. In addition to the cone geometry (i.e., cone length and diameter) four material constants (i.e., cohesion, angle of internal friction, density, and shear modulus) are needed to completely define a problem. This is an improvement over the existing cone penetration models that treat the soil as a rigid plastic medium considering only the shear strength of the material and neglecting its stiffness characteristics. Experimental data indicate that cone index does not depend solely on shear strength of the soil but also depends on the stiffness characteristics of the material (particularly for sand). The concept of free-surface effect for granular materials has been advanced and quantified for the WES cone.

19. It is recommended that a series of laboratory-controlled tests using cones of various apex angles and base areas be conducted in order to (a) evaluate the range of application of the model and (b) determine the feasibility of obtaining the engineering properties of soil (such as C , ϕ , G , and γ) from results of cone penetrometer measurements.

REFERENCES

1. Rula, A. A. and Nuttall, C. J., Jr.; "An Analysis of Ground Mobility Models (ANAMOB)"; Technical Report M-71-4, July 1971; U. S. Army Engineer Waterways Experiment Station, CE, Vicksburg, MS.
2. Yong, R. N. and Olen, C. K.; "Cone Penetration of Granular and Cohesive Soils"; Journal of the Engineering Mechanics Division, ASCE, EM2, April 1976.
3. Karafiath, L. L. and Nowatzki, E. A.; "Soil Mechanics in Off-Road Vehicle Engineering"; Trans Tech Publications, Bay Village, OH, 1976.
4. Vesic, A. S.; "Expansion of Cavities in Infinite Soil Mass"; Journal of the Soil Mechanics and Foundations Division, ASCE, Vol 98, SM3, Proc. Paper 8790, March 1972.
5. Baligh, M. M., Vivatrat, V., and Ladd, C. C.; "Exploration and Evaluation of Engineering Properties for Foundation Design of Offshore Structures"; MITSG 79-8, April 1979; Massachusetts Institute of Technology, Cambridge, MA.
6. Smith, J. L.; "Strength-Moisture-Density Relations of Fine-Grained Soils in Vehicle Mobility Research"; Technical Report No. 3-639, January 1964; U. S. Army Engineer Waterways Experiment Station, CE, Vicksburg, MS.
7. Melzer, K. J.; "Measuring Soil Properties in Vehicle Mobility Research, Report 4, Relative Density and Cone Penetration Resistance"; Technical Report No. 3-652, July 1971; U. S. Army Engineer Waterways Experiment Station, CE, Vicksburg, MS.

APPENDIX A: TREATMENT OF LAYERED SOIL

1. The cone penetration model can be readily extended to predict cone index (CI) in a layered system with each layer possessing distinct material properties. In principle it is feasible to develop an expression for CI in a multilayered system where the cone may be in contact with several layers at the same time. However, because of the size of the cone (i.e., being small in comparison with the thickness of typical soil layers encountered in nature), it is reasonable to assume that the cone may not be in contact with more than two distinct layers at the same time. This indicates that the thickness of each layer must be equal to or greater than the length of the cone. Figure A1 depicts the geometry of the problem where the cone is in contact with two distinct layers, n and $n+1$. The expressions for CI for the layered system in Figure A1 are similar to Equations 7 through 9. The material properties C , ϕ , \tilde{G} , and γ , however, must be properly indexed to reflect the location of the cone in the layered system. Whenever the cone is in contact with one layer (e.g., the generic layer i in Figure A1) the material properties C , ϕ , and \tilde{G} would correspond to C_i , ϕ_i , and \tilde{G}_i , respectively. The subscript i denotes the properties of layer i . The density γ , which represents the effect of the in situ hydrostatic stress (see Equation 4) on penetration resistance, can be replaced by an effective density accounting for the unit weight of all the layers above the tip of the cone

$$\gamma = \frac{\sum_{j=1}^{i-1} \gamma_j T_j + \left(L + Z - \sum_{j=1}^{i-1} T_j \right) \gamma_i}{L + Z} \quad (A1)$$

In Equation A1, T_j and γ_j denote the thickness and the density of the j th layer, respectively. When the cone crosses an interface (e.g., going from layer n to layer $n+1$ (Figure A1)), the material constants C , ϕ , \tilde{G} , and γ take the following forms

$$C = \frac{\left(L + Z - \sum_{j=1}^n T_j \right) C_{n+1} + \left(\sum_{j=1}^n T_j - z \right) C_n}{L} \quad (A2)$$

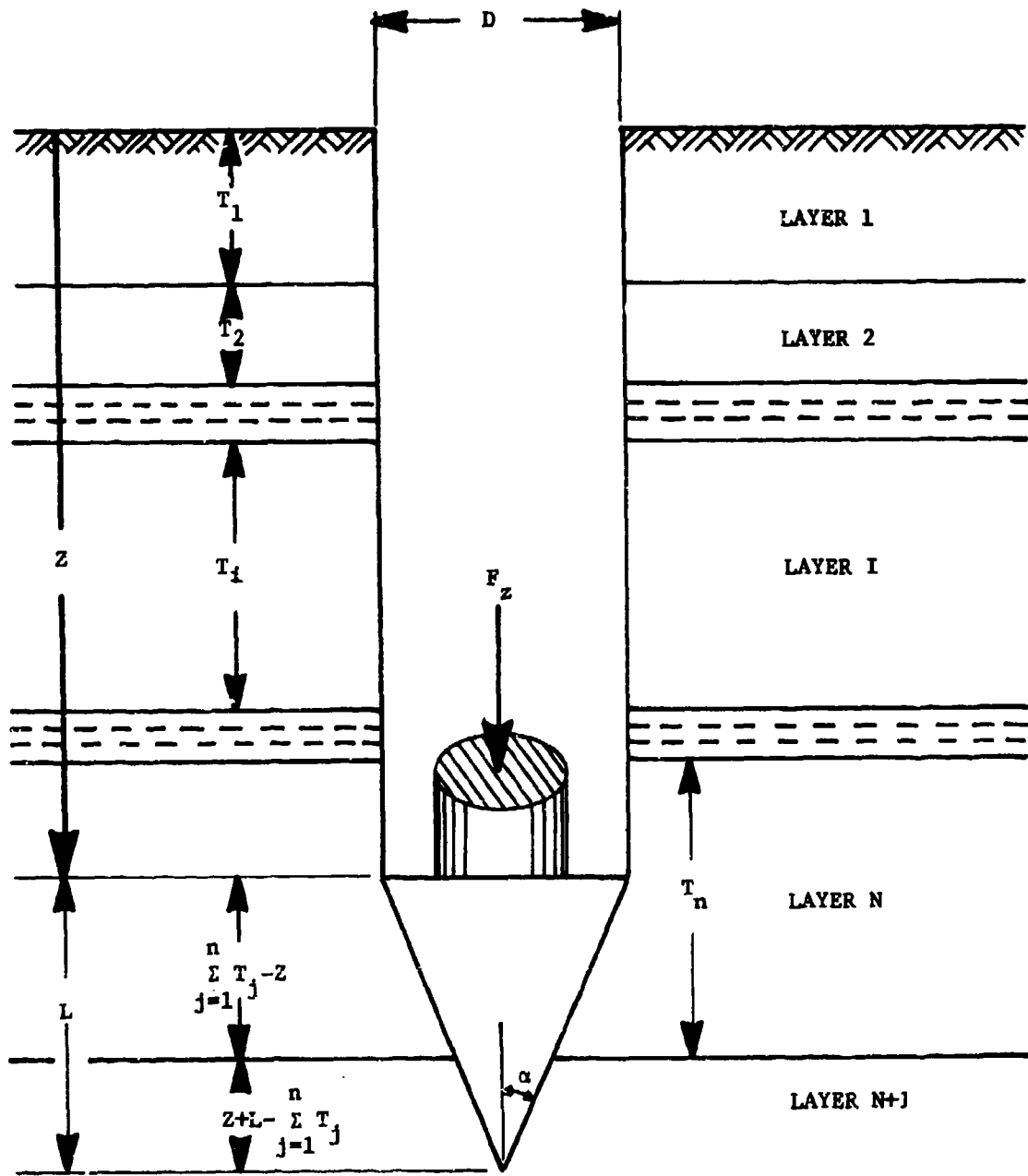


Figure A.1 Cone in contact with two layers.

$$\phi = \frac{\left(L + z - \sum_{j=1}^n T_j \right) \phi_{n+1} + \left(\sum_{j=1}^n T_j - z \right) \phi_n}{L} \quad (A3)$$

$$\tilde{G} = \frac{\left(L + z - \sum_{j=1}^n T_j \right) \tilde{G}_{n+1} + \left(\sum_{j=1}^n T_j - z \right) \tilde{G}_n}{L} \quad (A4)$$

$$\gamma = \frac{\sum_{j=1}^n \gamma_j T_j + \left(L + z - \sum_{j=1}^n T_j \right) \gamma_{n+1}}{L + z} \quad (A5)$$

It is noted from Equations A2 through A5 that the material properties C , ϕ , \tilde{G} , and γ are not constant but vary with depth as the cone crosses the interface and becomes fully embedded in layer $n+1$. When the cone is fully embedded in layer $n+1$, C , ϕ , and \tilde{G} reduce to C_{n+1} , ϕ_{n+1} , and \tilde{G}_{n+1} , respectively, and γ becomes the effective density consistent with Equation A1.

2. In order to demonstrate the application of Equations A1 through A5 in predicting CI in a layered system two example problems are given in this appendix using the standard WES cone. In the first example a layered clay soil consisting of five layers having the properties given in Table A1 is considered. It is noted from Table A1 that the material properties consistently increase with depth. The second example considers a layered soil consisting of three layers with the properties given in Table A2.

3. The result of the CI calculation for example problem 1 is shown in Figure A2 in terms of CI versus depth of penetration Z . As indicated in Figure A2, the depth of penetration Z is measured from the base of the cone (consistent with experimental measurements). Consistent with the properties given in Table A1, Figure A2 indicates that CI increases with the depth of penetration as the cone perforates each layer. Within each layer, however, CI is constant for a distance equivalent to the thickness of the layer minus the length of the cone. As the cone crosses an interface, the value of CI changes with depth until the base of the cone touches the interface. Figure A3 depicts the result of the CI calculation for example problem 2. The CI versus depth of penetration relation in Figure A3 is

Table A1
Soil Properties for Example Problem 1

<u>Layer No.</u>	<u>Layer Thickness in.</u>	<u>Cohesion lb/in.²</u>	<u>Density lb/in.³</u>	<u>Shear Modulus lb/in.²</u>
I	3	1	0.055	700
II	3	3	0.058	1000
III	4	5	0.060	2000
IV	5	7	0.063	2500
V	5	9	0.066	3000

Table A2
Soil Properties for Example Problem 2

<u>Layer No.</u>	<u>Layer Thickness in.</u>	<u>Cohesion lb/in.²</u>	<u>Friction Angle deg</u>	<u>Density lb/in.³</u>	<u>Shear Modulus lb/in.²</u>
I	5	1	30	0.060	1000
II	5	5	35	0.065	2500
III	10	0.5	25	0.060	700

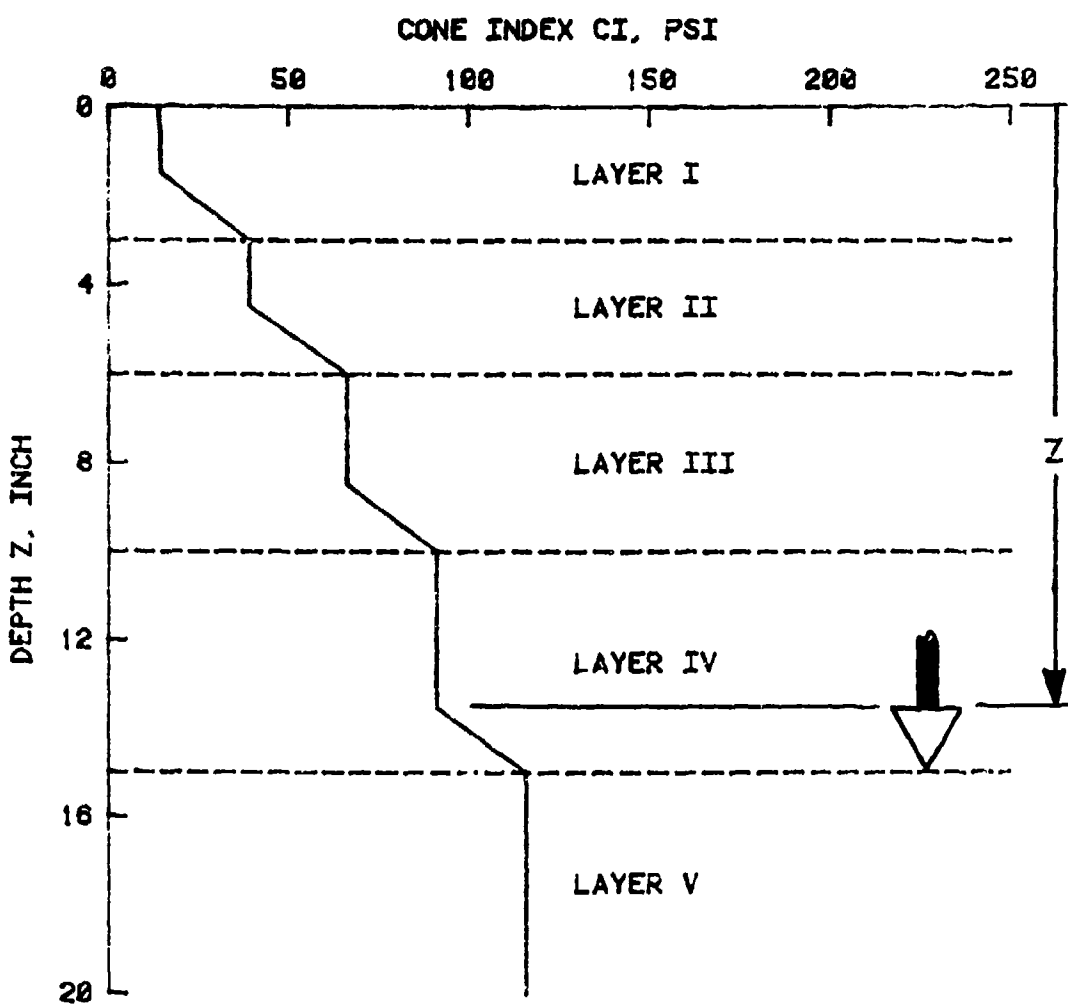


Figure A.2 Calculated cone index versus depth of penetration for example problem 1.

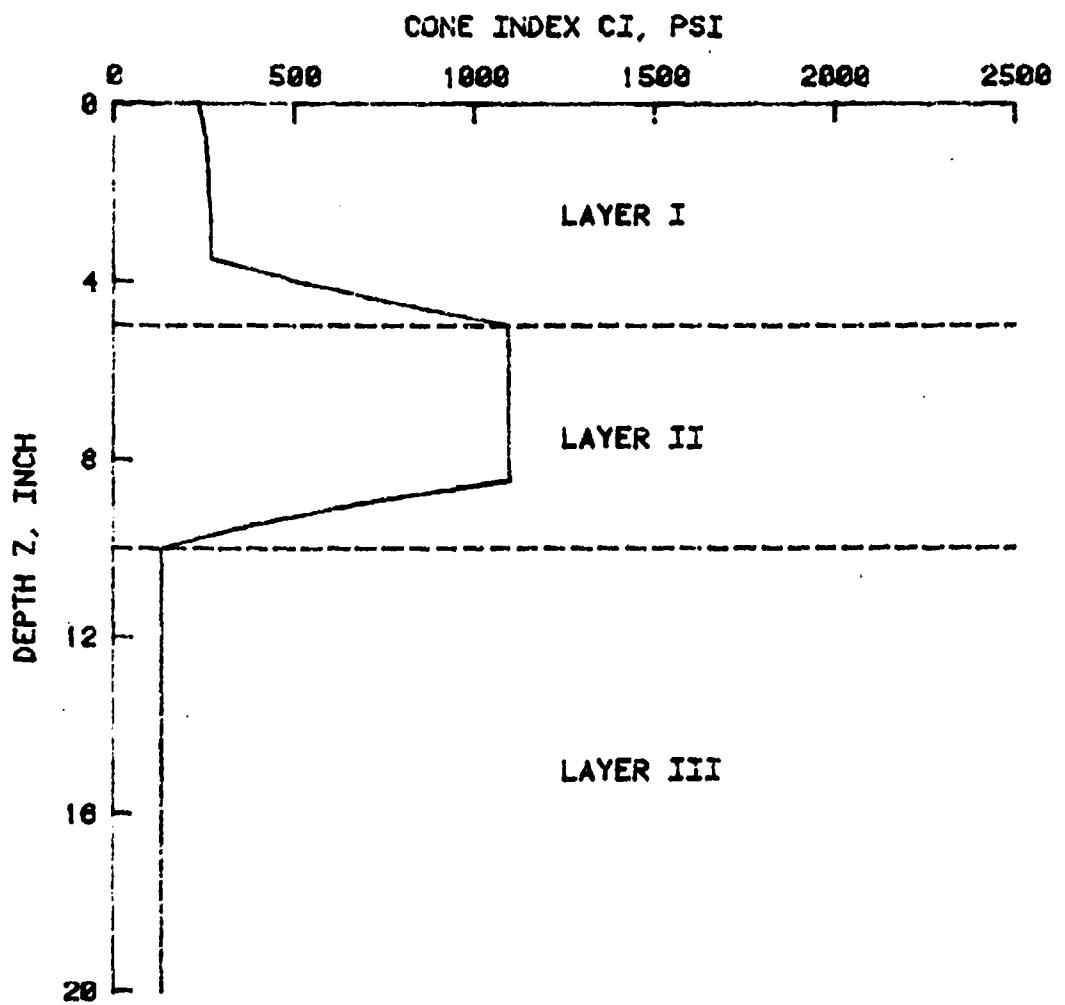


Figure A.3 Calculated cone index versus depth of penetration for example problem 2.

consistent with the properties given in Table A2. The value of CI increases as the cone crosses the interface between layers I and II (i.e., crossing from a soft layer to a hard layer). In layer II, CI is constant up to a depth of 8.52 in. and then decreases as the cone crosses the interface between layers II and III (i.e., crossing from a hard layer to a soft layer).

APPENDIX B: NOTATION

The following symbols are used in this paper:

- A = coefficient related to free-surface effect
- B = coefficient related to free-surface effect
- C = cohesion
- CI = cone index
- D = diameter of the cone
- F_z = vertical force resisting the penetration of the cone
- g = gravitational acceleration
- \tilde{G} = apparent shear modulus
- G = elastic shear modulus
- L = length of the cone
- q = in situ hydrostatic stress
- v_s = shear wave velocity
- Z = depth of penetration
- 2α = apex angle of the cone
- β = coefficient related to the free-surface effect
- γ = density
- σ = normal stress
- τ = shear stress
- ϕ = angle of internal friction

In accordance with letter from DAEN-RDC, DAEN-ASI dated 22 July 1977, Subject: Facsimile Catalog Cards for Laboratory Technical Publications, a facsimile catalog card in Library of Congress MARC format is reproduced below.

Rohani, Behzad

Correlation of mobility cone index with fundamental engineering properties of soil : final report / by Behzad Rohani, George Y. Baladi (Structures Laboratory, U.S. Army Engineer Waterways Experiment Station.) -- Vicksburg, Miss. : The Station, 1981.

36 p. in various pagings : ill. ; 27 cm. -- (Miscellaneous paper / U.S. Army Engineer Waterways Experiment Station ; SL-81-4.)

Cover title.

"Prepared for Office, Chief of Engineers, U.S. Army, under Project 4A161102AT22, Task CO, Work Unit 001."

"Monitored by Geotechnical Laboratory, U.S. Army Engineer Waterways Experiment Station."

"This paper was prepared for presentation at the Seventh International Congress of the International Society for Terrain-Vehicle Systems, 16-20 August 1981, Calgary, Canada. Paper is available from National Technical Information Service, Springfield, Va. 22161."

Rohani, Behzad

Correlation of mobility cone index : ... 1981.
(Card 2)

Bibliography: p. 28.

1. Mathematical models. 2. Penetrometer. 3. Soil penetration test. 4. Tracklaying vehicles. I. Baladi, George Y. II. United States. Army. Corps of Engineers. Office of the Chief of Engineers. III. United States. Army Engineer Waterways Experiment Station. Structures Laboratory. IV. Title V. Series: Miscellaneous paper (United States. Army Engineer Waterways Experiment Station) ; SL-81-4. TA7.W34m no.SL-81-4